VILNIUS UNIVERSITY

CENTER FOR PHYSICAL SCIENCES AND TECHNOLOGY
INSTITUTE OF CHEMISTRY

Tatjana Maliar

Synthesis of Iron particles in the aqueous and oil media and their application in the tribological systems

Summary of doctoral dissertation

Physical sciences, chemistry (03 P)

Vilnius, 2012

The work was carried out in Vilnius University in the period of 2008–20112.

Scientific supervisors:

Doc. dr. Ernestas Gaidamauskas 2007–2008 (Vilnius University, Physical sciences, Chemistry - 03P);

Prof. dr. Henrikas Cesiulis 2008–2011 (Vilnius University, Physical sciences, Chemistry - 03P);

Chairman:

Prof. dr. habil. Aivaras Kareiva (Vilnius University, Physical sciences, Chemistry 03P);

Members:

Prof. habil. dr. Arūnas Ramanavičius (Vilnius University, Physical sciences, Chemistry – 03P)

Prof. habil. dr. Albertas Malinauskas (Institute of Chemistry Center for Physical Sciences and Technology, Physical sciences, Chemistry – 03P)

Prof. habil. dr. Algimantas Undzėnas (Physics Institute Center for Physical Sciences and Technology, Physical sciences, Physics – 02P)

Dr. Natalia Tintaru (Catholic University of Leuven, Belgium, Physical sciences, Chemistry – 03P)

Opponents:

Prof. habil. dr. Rimantas Ramanauskas (Institute of Chemistry Center for Physical Sciences and Technology, Physical sciences, Chemistry – 03P)

Doc. dr. Audrius Žunda (Aleksandras Stulginskis University, Technological sciences, Mechanical Engineering – 09T)

The official discussion will be held at 2 p.m. on June 08, 2012 at the Auditorium of Inorganic Chemistry of the Chemistry Faculty of Vilnius University.

Address: Naugarduko 24, LT–03225 Vilnius, Lithuania.

Tel.: 231 15 72. Fax.: 233 09 87.

The summary of doctoral dissertation was mailed on the 07 of May 2012.

The dissertation is available at the Library of Vilnius University and the Library of Institute of Chemistry.

VILNIAUS UNIVERSITETAS

FIZINIŲ IR TECHNOLOGIJOS MOKSLŲ CENTRO CHEMIJOS INSTITUTAS

Tatjana Maliar

Geležies dalelių sintezė vandens ir alyvos terpėse ir jų taikymas tribosistemose

Daktaro disertacijos santrauka

Fiziniai mokslai, chemija (03 P)

Vilnius, 2012

Disertacija rengta 2008–2012 metais Vilniaus universitete.

Mokslinis vadovas:

Doc. dr. Ernestas Gaidamauskas 2007–2008 (Vilniaus universitetas, fiziniai mokslai, chemija - 03P);

Prof. dr. Henrikas Cesiulis 2008–2011 (Vilniaus universitetas, fiziniai mokslai, chemija – 03P);

Pirmininkas:

Prof. habil. dr. Aivaras Kareiva (Vilniaus universitetas, fiziniai mokslai, chemija – 03P);

Nariai:

Prof. habil. dr. Arūnas Ramanavičius (Vilniaus universitetas, fiziniai mokslai, chemija – 03P)

Prof. habil. dr. Albertas Malinauskas (Fizinių ir technologijos mokslų centro Chemijos institutas, fiziniai mokslai, chemija – 03P)

Prof. habil. dr. Algimantas Undzėnas (Fizinių ir technologijos mokslų centro Fizikos institutas, fiziniai mokslai, fizika – 02P)

Dr. Natalia Tintaru (Katališkasis Leuveno universitetas. Belgija, fiziniai mokslai, chemija – 03P)

Oponentai:

Prof. habil. dr. Rimantas Ramanauskas (Fizinių ir technologijos mokslų centro Chemijos institutas, fiziniai mokslai, chemija – 03P)

Doc. dr. Audrius Žunda (Aleksandro Stulginskio universitetas, technologijos mokslai, mechanikos inžinerija – 09T)

Disertacija bus ginama viešame Chemijos mokslo krypties tarybos posėdyje 2012 m. Birželio 08 d. 14 val. FTMC Vilniaus universiteto Chemijos fakulteto Neorganinės chemijos auditorijoje.

Adresas: Naugarduko 24, LT-03225 Vilnius, Lietuva.

Tel.: 231 15 72. Fax.: 233 09 87.

Disertacijos santrauka išsiųsta 2012 m. Gegužės 07 d.

Su disertacija galima susipažinti Vilniaus universiteto ir Chemijos instituto bibliotekose.

Introduction

The reliability of machines and mechanisms mainly are defining by the friction processes in the kinematic pairs. For example, in automotive engines it is estimated that about 20–25 % of the generated energy by combustion is lost by the frictional dissipation. The wear defines up to 80–95 % of failures and damages of surfaces. Nowadays, many attempts are made to solve tribological issues by the adding of metallic and non–metallic powders in lubricants and oils. Nanoparticles are able to penetrate into all places of friction surfaces especially in deformations or microcracks. The main objective related with the usage of magnetic nanoparticles like Fe, Co, Ni is to minimize friction and wear in tribocontact. However, an unavoidable problem of wide practical usage of magnetic nanoparticles (Fe, Ni, Co, their alloys) in various fields included tribology associated with particles in this size range is their intrinsic instability over longer periods of time. Such small particles tend to form agglomerates to reduce the energy associated with the high surface area to volume ratio. Moreover, "naked" metallic nanoparticles are chemically extremely active, and are easily oxidized in air or other media, resulting in loss of magnetism and dispersity. Therefore, it is crucial to develop protection strategies of stabilization the naked magnetic nanoparticles against degradation during or after the synthesis. These strategies comprise coating with organic species, including surfactants and polymers or modification the surface by the more noble metals. This leads to form magnetic core and noble shell. The metals able to form a shell might be following: Au, Pt, Zn, Cu, Ag, and polymeric compounds. On the other hand, these tasks also comprise necessity to use modified nanoparticles, to develop methods and technologies in order to obtain nanoparticles of desired size and phase content.

Novelty of scientific investigation:

Due to increasing demand for oil and stringent environmental laws, the on–going trend in lubricant industry is to explore oils from renewable resources, such as vegetables. From the ecological point of view it is important that up to 15 % of used oil recycled into environment and causes the pollution of nature. Therefore, it is important to reduce pollution by using biologically degradable grades of oils. Vegetable oils usually possess attractive properties like biodegradability, low volatility, and good rheology in comparison with the conventional mineral or synthetic oils without functional additives. Moreover, vegetable oils stand out for its low friction and anti–wear property. Usually each lubricant contains friction modifiers and anti–wear additives to protect surfaces under the boundary lubrication conditions. It has been noticed that traditional lubricant additives are better suited for mineral oils than for vegetable. Hereto, there is the on–going research towards novel additives suitable for the vegetable and other biodegradable oils. Thus, when evaluating the influence of new chemical systems on friction and wear, it is rational to compare their effectiveness in mineral oils and vegetable oils. Since even without the additives the vegetable oils demonstrate better lubricating properties, this effect can be even more pronounced when nanoparticles are introduced. On the other hand, during friction the metallic debris are generated and can contaminate oil and also can affect its exploitation properties. Therefore, the data collection about tribological behavior of debris or metallic particles–contaminated

lubricants has a practical interest and increase the knowledge of the behaviour of real tribosystems.

The main aims of the work were followings:

1. To synthesize iron particles in aqueous medium and reverse micelles in SAE 10 mineral and rapeseed oil phases by colloidal technique in the presence of surfactants and evaluate sizes of obtained iron particles.
2. To study electrochemical aspects of the synthesis and transmetallization ("cementation") of iron particles by copper.
3. To create the methodology for corrosion investigation of iron particles in oils.
4. To investigate the effect of synthesized Fe particles as additives on the lubricating properties of commercially available SAE 10 mineral and rapeseed oils under relatively high and low loads.

Statements for defense:

1. The preparation of suspensions with Fe particles, its stabilization and size distribution of obtained Fe particles is described in colloidal chemistry terms.
2. The transmetallization of Fe by copper occurs as long as copper ions are presented in the solution. The used surfactants for stabilization of Fe particles do not prevent the cementation reaction; they only decrease copper ions reduction rate.
3. Corrosion rates of iron particles in rapeseed and SAE 10 mineral oils correlate both with size distribution of iron particles and whole composition of produced suspensions.
4. The efficiency of significant decrease of wear and friction losses of the surfaces in most cases relates both with produced Fe particles and whole composition of used suspensions, i.e., rapeseed/mineral oil + surfactant + Fe particles.

2. EXPERIMENTAL

2.1. Reagents and solutions, analysis of obtained particles

Analytical grade chemicals and distilled water were used to prepare solutions. The pH of the solution was controlled using pH–meter by adding concentrated H_2SO_4 or NaOH.

An antioxidant 0.5 wt % octadecyl–3–(3',5'–di–t–butyl–4–hydroxyphenyl) propionate was added to rapeseed oil (RO) and SAE 10 mineral oil (MO) immediately after receiving from the supplier.

For protection of produced suspensions against sedimentation and agglomeration the following surfactants were used: glycerol dilaurate GLY G2L (GLY), block copolymer ENB 90R4 (ENB), oxyethylated alcohol OS–20 (OS) and lanolin FVE VO2 (FVE). Prior the synthesis surfactants were dissolved in aqueous media, rapeseed and mineral oils at the temperature of 50–60 ^{0}C and cooled down. Then synthesis of iron particles was performed at room temperature.

Sizes of iron particles were measured by Dynamic Light Scattering (DLS) under ambient conditions using Zetasizer Nano S equipment (Malvern Instruments).

The morphology of iron particles was investigated by scanning electron microscopy (JEOL JSM–5600 and Hitachi Oxford Instruments FE–SEM SU70). X-ray diffraction analyses were performed by a Dron (type 3.0) instrument with Ni filtered Cu-$K_{\alpha 1}$ radiation operated at 30 kV and 30 mA (λ=1.54056 Å) was used at continuous scan speed of 0.02^0 2θ s^{-1}.

2.2. Determination of Fe corrosion rates by spectrophotometric analysis

Corrosion rates of Fe particles in the rapeseed and SAE 10 mineral oils were determined based on the determined concentrations of Fe (II) and Fe (III) in the solution. For this purpose the optical density of solutions containing sulfosalycylic acid was measured using a КФК-2МП spectrophotometer. The concentrations range was selected based on the 0.1 wt % Fe metallic particles produced in oil phases. Prior analysis iron particles were separated from oil phases by heptane. Test samples for spectrophotometric analysis were prepared in this way. In a 50 mL flask added a certain amount of standard $FeSO_4$ solution (18; 36; 72; 144 and 288 μL), then added 1 mL of 20 % sulfosalicylic acid, diluted them with distilled, and mixed thoroughly. Absorbance measurements are carried out at the wavelength λ=490 nm.

2.3. Measurements of kinematic viscosity

A kinematic viscosity of the oil solutions was measured at 22±1 and 75±1 ^{0}C by Ostvald type capillary viscometer VPZ-2 (Russia) with a diameter of capillary 1.77 mm. The viscosity was determined using following equation provided by the manufacturer:

$$v = \frac{g}{9.807} \cdot t \cdot K \qquad (1),$$

where v is a kinematic viscosity of investigating liquid (mm^2 s^{-1}); g is a gravity factor (m s^{-2}); t is drainage time of investigated liquid (seconds); K is a constant of particular viscometer issued by the manufacturer (for this viscometer K=1.088 mm^2 s^{-2}).

2.3. Electrochemical measurements

The electrochemical investigations were carried out using AUTOLAB N302 system at 20±2 ^{o}C. Linear sweep voltammetry were performed using 0.002 V s^{-1} potential scan rate. Measurements were carried out in a three-electrode cell with saturated silver chloride electrode as the reference, Pt wire netting was served as a counter electrode, and Fe electrode (99.99 % Alfa Aesar) and Cu (99.99 % Alfa Aesar) as working electrodes (working area 0.008 and 0.04 cm^2, respectively). All values of potential are presented against the saturated silver chloride reference electrode. Before each experiment Fe and Cu electrodes were mechanically polished with 2500 grid paper and rinsed in distilled water.

2.4. Tribological tests

2.4.1. Four-Ball Wear tribotest under high loads

For this study a Four-Ball Wear tribotester (Falex Corporation, the U.S.) was used. The test set-up consists of a 12.7 mm diameter top steel ball rotating in the cavity of three identical steel balls in contact which remain clamped in a cup containing the lubricant. Thus the Four-Ball Wear test assembly creates a three-point contact by the top ball. The desired load is applied from the bottom pneumatically, and the top ball is rotated at a preset speed and duration. The friction between the balls is measured by a

load cell connected to the bottom cup containing three balls. Each test requires about 15-20 ml lubricant. Before each experiment the steel balls (100Cr6 steel) were thoroughly cleaned in heptane and ethanol. The experimental parameters are listed in Table 1. All the three experiments were duplicated and the results were averaged.

Table 1. Test conditions applied in Four-Ball Wear tribotest

Material	Ø 12,7 mm bearing balls of steel 100Cr6
Load, N	392 and 588
Time, h	1 and 2
Rotating speed, rpm	1200
Temperature, °C	75

The wear loss was estimated based on the circular wear scar diameters obtained on the three stationary balls after the test. The wear scar diameter was measured on the tested balls by the optical microscope (Axio, Carl Ziess Intruments, Germany).

The average coefficient of friction, $\bar{\mu}$, and wear loss, W_L, are estimated, respectively, by the following equations:

$$\bar{\mu} = 16.926 \frac{F_t}{1000 \cdot L} \qquad (2)$$

where $\bar{\mu}$ - the average coefficient of friction, F_t - a friction torque (g), L - a load (Kg).

$$W_L = 3.14 \cdot (W_1^2 + W_2^2 + W_3^2) \qquad (3)$$

where W_L - the wear area (mm^2) and W - the average wear scar diameter (mm).

2.4.2. MUST tribotests under low loads

The reciprocating sliding tests under normal forces in milliNewtons range were performed with a high precision microtribometer (MUST, Falex Tribology NV, Belgium) in a ball-on-flat contact configuration. The MUST equipment detects the cantilever deflection either in tangential or normal direction by light optical sensors. The counterbody is glued at tip of this cantilever and the sample to be tested is placed on a reciprocating table. The relative position of the counterbody and sample can be altered by means of fully automated positioning controls. The chosen tribotest parameters are listed in Table 2.

Table 2. Test conditions for MUST reciprocating tribotest

Material	24 mm Ø AISI52100 steel discs 3.175 mm Ø 100Cr6 steel balls
Stroke length, mm	5
Normal force, mN	500, 750 and 900
Sliding speed, mm/s	0.05; 0.5 and 2.6
Number of cycles	50
Temperature, ^{0}C	23 ± 3

Both the disc and counterbody were thoroughly cleaned prior experiments to eliminate effects of contaminants in the friction measurements. Before each test 2-3 ml of the testing oil suspension was dropped on the disc and spread uniformly using a spatula. All these tests were duplicated and the average data was calculated.

The average coefficient of friction is calculated from the friction loops. The integrated area of each friction loop corresponds to the dissipated energy, E_d, during one

reciprocating cycle. The dissipated energy calculated for a particular cycle is equal to $\int F_t \, dx$, with F_t - the immediate tangential force. The average coefficient of friction, $\bar{\mu}$, is estimated by the equation:

$$\bar{\mu} = \frac{E_d}{2 \cdot F_N \cdot s} \qquad (4)$$

where F_N is the normal force (N), and s is the net sliding distance (mm), which is equal to the length of the gross slip during the displacement in one direction.

3. RESULTS AND DISCUSSION

3.1. Iron particles synthesis in water and oil phases

3.1.1. Selection of surfactants

The optimal concentrations of surfactants were selected based on the suspensions stability results provided by Dr. S. J. Asadauskas group (Institute of Chemistry Center for Physical Sciences and Technology). Concentrations of surfactants (GLY G2L glycerol dilaurate, ENB 904R block copolymer, FVE VO2 lanolin) were varied by 3-3.5 times to evaluate their effect on the suspension stability. The results show that the most optimum concentrations of surfactants are: 10 wt % GLY; 0.5 wt % ENB; and 10 wt % FVE. Additional measurements with OS ethoxylated alcohol were performed. It is noticed that the most favourable concentration of OS was 0.5 wt %.

In agreement with classical colloid theory, surfactant adsorbs on the metal/water or micelle/oil interfaces. It stabilizes the suspension or improves the suspension stability by two main electrostatic repulsion and steric repulsion mechanisms. Electrostatic stability of suspension is provided by the adsorption of anionic surfactant on metal/water or micelle/oil interfaces and formed an electrically charged layer - shell. The formed charged positively/negatively layer prevents particles or micelles from agglomeration or coalescention. Steric repulsion mechanism is based on the principle of surfactant adsorption on the particle surface as well. Relatively rigid molecular fragments of surfactant thrust up into liquid and repulse the agglomeration with other particles. There is other more exotic mechanism of stabilization, such as a formation of gel-like network. The agglomeration and sedimentation of particles is impeded by formation of viscous medium as a gel structure.

3.1.2. Iron particle synthesis in water

There were two reducing agents used for obtaining iron particles: sodium borohydride $NaBH_4$ and lithium triethylborohydride $LiB(C_2H_5)_3H$.

a) The usage of $NaBH_4$ reducing agent

Sodium borohydride $NaBH_4$ and ferric sulphate $FeSO_4$ were used as precursors for the synthesis of iron particles. The synthesis was performed by wet chemical reaction by colloidal technique in water containing the antioxidant without/with one of surfactants. 0,02 M $FeSO_4$ solution was added drop by drop to aqueous 0,04 M $NaBH_4$ solution containing the antioxidant without/with one of surfactants sufficient to obtain 0,1 wt % Fe particles. The correct amounts of sodium borohydride and ferric sulphate solutions were calculated based on the stoichiometry of the reduction-oxidation reaction:

$$Fe^{2+} + 2BH_4^- + 6H_2O \xrightarrow{\pm 2e^-} Fe^0_{(s)} + 2H_2BO_3^- + 4H^+ + 6H_{2(gas)} \qquad (1)$$

b) The usage of $LiB(C_2H_5)_3H$ reducing agent

1 M $LiB(C_2H_5)_3H$ in tetrahydrofuran solution was added drop by drop to aqueous 0.7 M $FeSO_4$ solution containing the antioxidant without/with one of surfactant sufficient to obtain 0.1 wt % Fe particles. The correct amounts of $LiB(C_2H_5)_3H$ and $FeSO_4$ solutions were calculated based on the stoichiometry of the reduction-oxidation reaction:

$$Fe^{2+} + 2B(Et)_3H^- \xrightarrow{\pm 2e^-} Fe^0_{(s)} + 2B(Et)_3 + H_{2(gas)} \qquad (2)$$

The size distribution of obtained Fe particles in water using $NaBH_4$ and $LiBEt_3H$ as the reducing agents is shown in Fig. 1. In all investigated cases the obtained Fe particles are polydispersed (see Fig. 1).

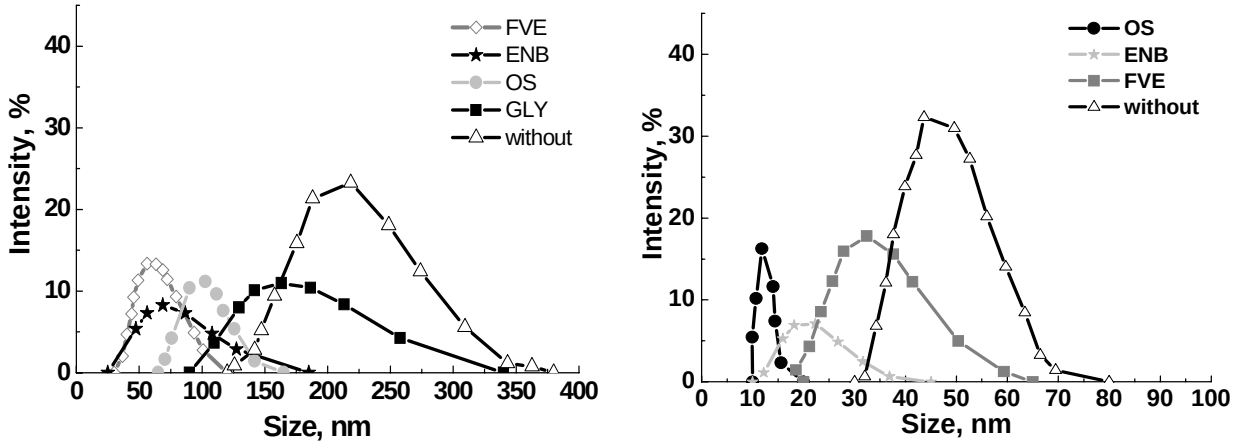

Fig. 1. The size distribution of Fe-particles obtained in aqueous solution using (a) $NaBH_4$ and (b) $LiB(C_2H_5)_3H$. Resulting concentration of Fe-particles is 0.1 wt %.

Fig. 1a illustrates the effect of various surfactants on the size distribution of iron particles obtained using $NaBH_4$. In this case the measured sizes of obtained Fe particles vary in a wide range from 25 to 380 nm. The most effective surfactant is 10 % FVE (the range of Fe particles size is 30-120 nm). The biggest iron particles were obtained in suspensions with 10 % GLY (90-340 nm) and without surfactant (120-380 nm).

However, as it shown in Figure 1b using $LiBEt_3H$ as reducing agent the obtained sizes of iron particles vary in significantly smaller range (10-80 nm). The biggest size distribution of iron particles is produced in aqueous suspension without surfactant, the smallest - with 0.5 % ENB and 0.5 % OS.

3.1.3. Electrochemical aspects of the synthesis of iron particles

a) Synthesis without surfactants

The reduction of hydrated Fe^{2+} ions to metallic Fe occurs in the presence of reducing agents that cause the shift of the open circuit potential (OCP) of Fe towards more negative potentials (Figs. 2 and 3). Both $NaBH_4$ and $LiBEt_3H$ shift the values of OCP dependently on its concentration: the higher concentration, the OCP shift towards negative values is bigger. The most negative values of OCP can reach up to –1.1 V in the presence of $NaBH_4$ (Fig. 2), and this compound influences on OCP much stronger than $LiBEt_3H$. The weighing values of OCP against corresponding positions on the polarization curves (Fig. 4) show that OCP values match the range in cathodic branch of polarization curve corresponding to the maximal rate of Fe^{2+} reduction in the presence of

$NaBH_4$, whereas OCP in the presence of $LiBEt_3H$ corresponds with inceptive range of Fe^{2+} reduction potentials at higher concentrations only. Those results in the different rates of appearing Fe-particles in course of reduction by $NaBH_4$ and $LiBEt_3H$ in aqueous medium, namely, in the presence of $NaBH_4$ iron particles form almost immediately, whereas in the presence of $LiBEt_3H$ iron particles appear within 30–60 minutes.

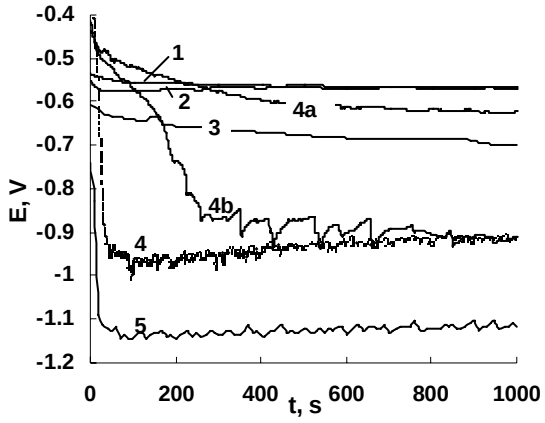

Fig. 2. OCP vs. immersion time of Fe-electrode in 0.5 M Na_2SO_4 (pH 3) with various additions of $NaBH_4$ or $FeSO_4$, (in mol L^{-1}): 1 – 0; 2–0.018 M $FeSO_4$; 3–0.0072 M $NaBH_4$; 4–0.036 M $NaBH_4$ (IV); 4a–IV + 0.5 wt % ENB 90R4; 4b–IV + 0.5 wt % OS-20; 5–0.18 M $NaBH_4$.

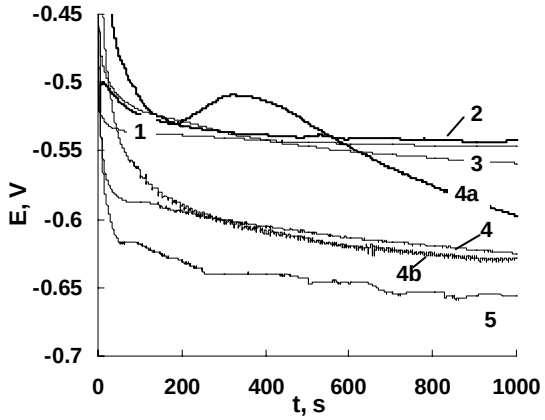

Fig. 3. OCP of Fe-electrode in 0.5 M Na_2SO_4 (pH 3) with various additions of $LiBEt_3H$ or $FeSO_4$, (in mol L^{-1}): 1–0; 2–0.018 M $FeSO_4$; 3–0.0072 M $LiBEt_3H$; 4–0.036 M $LiBEt_3H$ (IV); 4a –IV + 0.5 wt % OS-20; 4b–IV + 0.5 wt % ENB 90R4; 5–0.09 M $LiBEt_3H$.

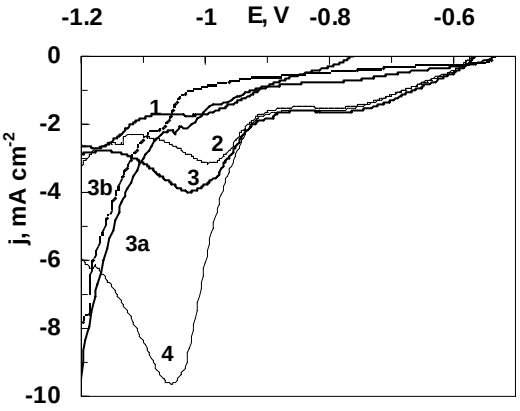

Fig. 4. Cathodic polarization curves of Fe-electrode in 0.5 M Na_2SO_4 solutions at pH 3 and containing various concentrations of $FeSO_4$: 1–0; 2–0.0036 M; 3–0.018 M (III); 3a–III + 0.5 wt % OS-20; 3b – III + 0.5 wt % Tetronic 90R4; 4 – 0.090 M.

The different rates of Fe^{2+} reduction to Fe^0 result the different sizes of obtained particles using these two reducers. If $NaBH_4$ acts as reducer, the sizes of Fe-particles obtained in water phase and reverse micelles without surfactants are substantially bigger (2–5 times). Some characteristic results are presented in Fig. 5.

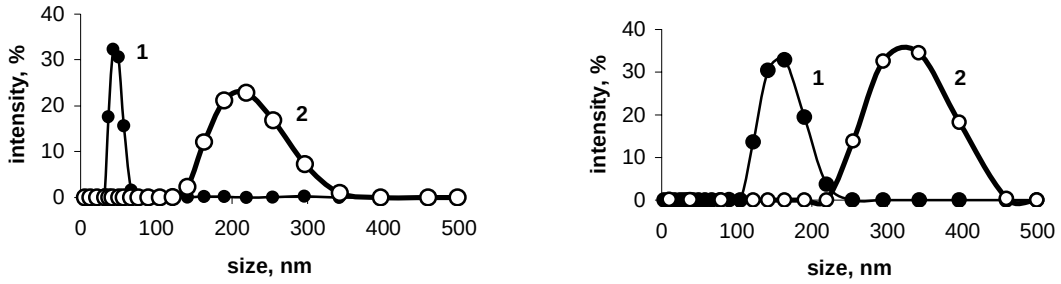

Fig. 5. The size distribution of Fe-particles obtained in aqueous solution (a) and the reverse micelles formed in the mineral SAE 10 oil (b) in the presence of $LiBEt_3H$ (1) and $NaBH_4$ (2). Resulting concentration of Fe-particles is 0.1 wt %.

The structure of obtained Fe-powder was studied by the X-ray diffraction method, and XRD pattern is shown in Fig. 6. It consists of one relatively wide peak attributed to the dominating structure {110} of body centred cubic lattice of metallic iron, which is formed in course of synthesis using $NaBH_4$. Also some unidentified peaks presence and their intensity are compatible with noise. Usually the structure of Fe particles is concerning as a typical core-shell structure. The core consists primarily of zero-valent or metallic iron while the mixed valent, i.e., Fe(II) and Fe(III) oxide shell is formed as a result of the oxidation of metallic iron. Probably, in this case the thickness of shell is too small in order to form a separate XRD peak representing oxide phase.

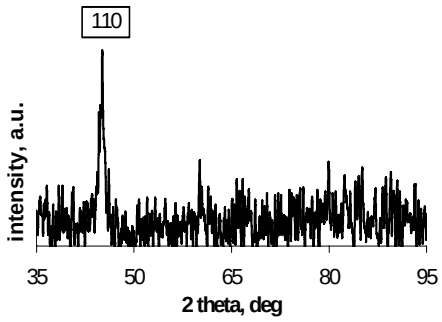

Fig. 6. XRD pattern of Fe powder followed synthesis by the reduction using $NaBH_4$ as reducing agent in water phase and dried at room temperature.

b) The effect of surfactants

As it is shown in Figs. 2 and 3, the adding of surfactants change values of OCP of Fe-electrode (ENB with $NaBH_4$ and OS with $LiBEt_3H$), especially the rate of potential shift at the beginning of process. Also, due to adsorption of surfactant the values of polarization increase (see Fig. 4, curves 3a and 3b). The obtained values of OCP match the inceptive range of the cathodic branch polarization curve that correlates with decreased rate of particles formation. In the case of particles synthesis, surfactant presenting in the reaction mixture adsorbs and forms a protective shell around Fe-particles that prevents the agglomeration of Fe-particles. Therefore, in the presence of surfactants the size of obtained particles decreases down to nanometer level in water phase (see Fig. 7).

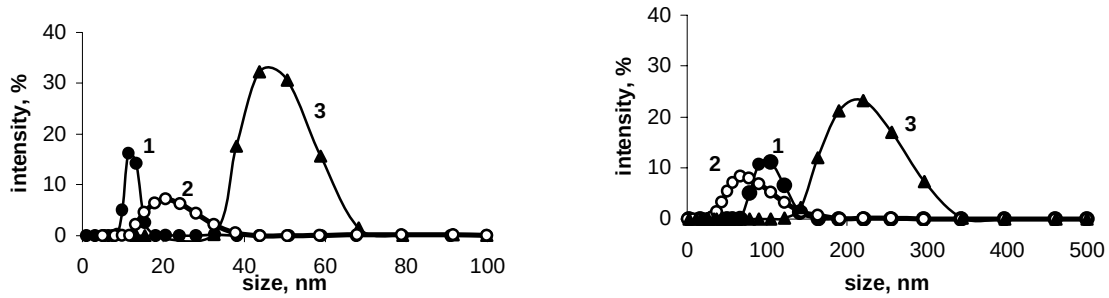

Fig. 7. The size distribution of Fe particles obtained in water and with adding surfactants: OS-20 (1), ENB 90R4 (2) and without surfactant (3) in the presence of $LiBEt_3H$ (a) and $NaBH_4$ (b). Resulting concentration of Fe particles is 0.1 wt%.

When Fe-particles are synthesized in the reverse micelles in oil phase, the surfactant molecules can adsorb both on Fe/oil and micelle/oil interfaces. In the last case, due to adsorption of surfactant the interfacial tension is lowering, and micelles containing Fe^{2+} and reducing agent can easier to coalescent during stirring. Moreover, the adsorption of surfactant facilitates the coalescention of released Fe particles and micelles. Both this factors increase the rate of forming and size of resulting Fe-particles under electrochemical mechanism. On the other hand, adsorbed surfactants form the shells that mechanically prevent the agglomeration of synthesized Fe-particles or prevent the coalescention of micelles, and conditions of synthesis are complicated due to the electrochemical and steric stabilization occurring simultaneously. Therefore, the effect of surfactants on the sizes of Fe-particles becomes unpredictable in advance. This point of view is well illustrated by the data shown in Fig. 8.

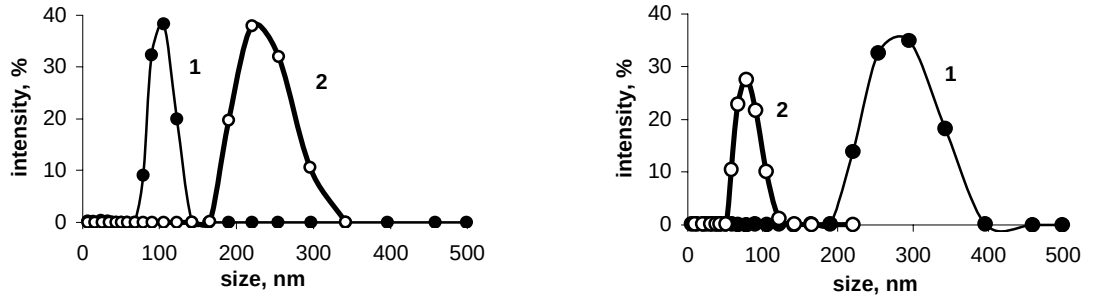

Fig. 8. The size distribution of Fe particles obtained in the reverse micelles formed in (a) the rapeseed oil with added Tetronic 90R4 and (b) the mineral SAE-10 oil with OS-20 and in the presence of $LiBEt_3H$ (1) and $NaBH_4$ (2). Resulting concentration of Fe particles is 0.1 wt%.

The size of Fe-particles synthesized either in water or oil phases without surfactants using $LiBEt_3H$ are less than using $NaBH_4$ because of electrochemical factors (see Figs. 5, 7 and 8a), but by varying oils and surfactants due to dominating steric stabilization mentioned above, it is possible to obtain opposite result: the size of Fe-particles obtained using $NaBH_4$ are less than using $LiBEt_3H$ (see Fig. 8b).

3.1.4. Synthesis of iron particles in the rapeseed and SAE 10 mineral oils

a) The usage of $NaBH_4$ as reducing agent

The synthesis of iron particles was performed by wet chemical reaction in reverse micelles (colloidal technique) in the oil phase containing the antioxidant without/with one of surfactants. In order to reduce the amount of water in the suspensions of the

rapeseed oil (RA) and SAE 10 mineral oil (MO) initial $NaBH_4$ and $FeSO_4$ concentrations were significantly increased. In this way, the amount of water in the final suspension did not exceed 4.4 %.

The relevant aqueous solution amounts of 1.4 M $NaBH_4$ and 0.7 M $FeSO_4$ were added to the corresponding RO or MO containing the antioxidant and the surfactant sufficient to obtain 0.1 wt % Fe particles in the oils. Each component was added after vigorous stirring for 30 seconds using Vortex-type mixer. The correct amounts of sodium borohydride and ferric sulphate solutions were calculated from the reduction-oxidation reaction (1).

The size distributions of obtained Fe particles in the RO and MO using $NaBH_4$ as the reducing agent are shown in Fig. 9. It was noticed that in the RA with 10 % FVE iron particles oxidized shortly at the same rate as in the suspension without surfactant. The smallest size of Fe particles was obtained in the RO suspension with 0.5 % OS ethoxylated alcohol. In the RO suspensions with 0.5 % ENB and 10 % GLY surfactants the size distribution ranges of the obtained Fe particles are enough similar.

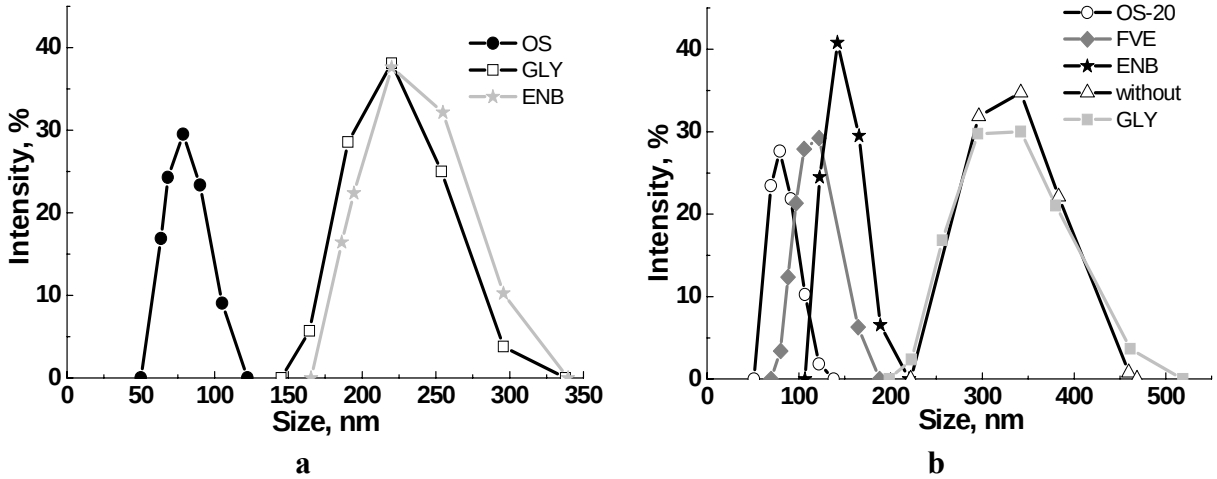

Fig. 9. The size distribution of Fe-particles obtained using $NaBH_4$ reducing agent in (a) rapeseed oil and (b) SAE 10 mineral oil. Resulting concentration of Fe-particles is 0.1 wt %.

The size distributions of produced Fe particles in the MO are presented in Fig. 9b. As it is seen, the size of Fe particles is distributed in a wide range from 50 to 530 nm dependently on surfactants used. The smallest iron particles are obtained in the MO suspension with 0.5 % OS, the biggest - with 10 % GLY and without surfactant.

b) The usage of $LiB(C_2H_5)_3H$ as reducing agent

The same preparation of suspensions was performed as in water (see 3.1.2. section).

The size distributions of obtained Fe particles in the RO and MO using $LiBEt_3H$ reducing agents are shown in Fig. 10. Similarly as using $NaBH_4$ to prepare Fe-containing suspension in RO (Fig. 9a), the same fast oxidation processes of Fe particles were observed using $LiBEt_3H$ as well. Ineffective in preparation of Fe particles was 0.5 % OS surfactant.

The size of Fe particles is distributed over a wide range from 105 to 825 nm (see Fig. 10b). The smallest size of Fe particles were produced in the MO without additives (105-255 nm). Slightly higher Fe particle sizes obtained with 10 % FVE (140-295 nm). The largest size of Fe particles was obtained in the MO with 10 % GLY (295-825 nm).

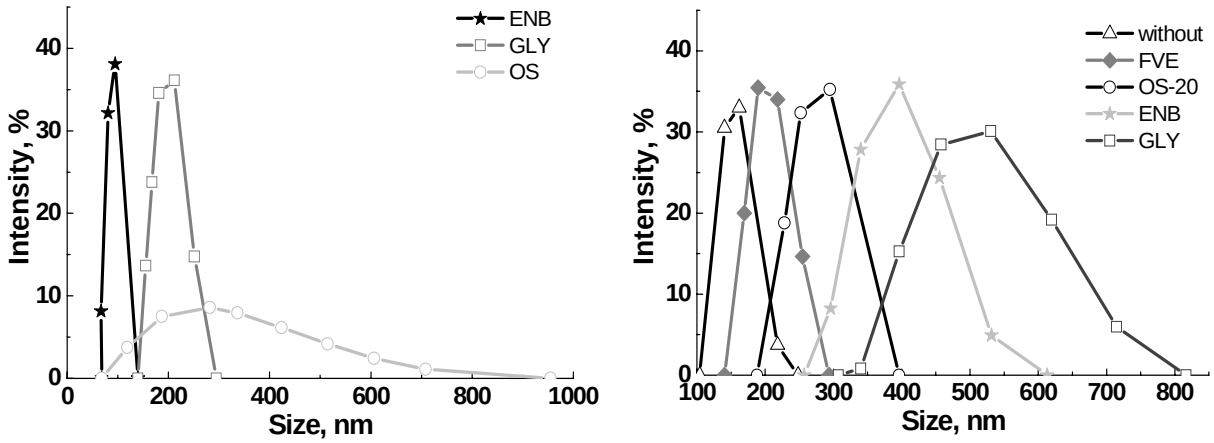

Fig. 10. The size distribution of Fe-particles obtained using reducing agent $LiB(C_2H_5)_3H$ in (a) rapeseed oil and (b) SAE 10 mineral oil. Resulting concentration of Fe-particles is 0.1 wt %.

Summarizing the obtained results it is possible to state:

- ✓ The using $LiBEt_3H$ results in smaller size of obtained Fe particles in water phase than using $NaBH_4$. This is due to Fe^{2+} ions reduction rate: the lower the reaction rate, the smaller particles are formed.
- ✓ The same range of the size of Fe particles was obtained using $NaBH_4$ and $LiBEt_3H$ reducing agents in the presence of surfactant GLY in the rapeseed oil. Furthermore, smaller Fe particles were obtained in the RO suspension with ENB by reduction of $LiBEt_3H$ than $NaBH_4$. Meanwhile, in the suspension with OS surfactant the opposite result was noticed. It could be explained by the simultaneous influence of electrochemical and steric repulsion stabilization factors, and the last one becomes dominating. In addition, the RA has stronger oxidizing properties than the MO. The oxidation of synthesized Fe particles in the RA suspensions with of FVE and without surfactant occurs rapidly.
- ✓ The size of Fe particles obtained in the MO using $NaBH_4$ are less than using $LiBEt_3H$, except for the suspension without added surfactant. In this case, probably due to adsorption of surfactant on micelle/oil interface the surface tension is lowering, and micelles containing Fe^{2+} and reducing agent can easier to coalescent during stirring. Moreover, the adsorption of surfactant facilitates the coalescention of released Fe-particles and micelles. Both this factors increase the rate of forming and size of resulting Fe-particles using $LiBEt_3H$ as reducing agent.

3.2. Electrochemical aspects of iron particles modification by copper

The cementation of iron by copper occurs via an electrochemical mechanism coupling reduction reaction

$$Cu^{2+} + 2e^{-} = Cu \qquad (3)$$

and oxidation reaction

$$Fe = Fe^{2+} + 2e^{-} \qquad (4)$$

occurring simultaneously. The overall reaction can be express as:

$$Fe_x + nCu^{2+} \xrightarrow[2ne^{-}]{\text{ligandai}} Fe_{x-n} - Cu_n + nFe^{2+} \qquad (5)$$

Thus, reaction (3) occurs according to the peculiarities of cathodic processes, and reaction (4) occurs according to the peculiarities of anodic processes. The rate of overall reaction (5) will correspond to the equality of the current densities of reactions (3) and (4) at a steady-state value of the stationary potential.

If the surface of iron is completely covered with Cu, i.e. becomes inaccessible for the occurrence of reaction (4), then the reaction of cementation of Fe by Cu would stop.

It is evident from Fig. 11 that the electroreduction of Cu^{2+} ions begins in the range of potential values of 0.05–0.1 V, the rate of the electroreduction reaction depends on the concentration of Cu(II) in the solution, and the limiting rate value varies in the range of 1.6 mA/cm^2 (0.008 M $CuSO_4$) to 78 mA/cm^2 (1 M $CuSO_4$). These results suppose that the limiting current density of electroreduction of Cu(II) is directly proportional to the concentration of $CuSO_4$ in the solution (Fig. 12). Slight deviations from the linear dependence can be attributed to the formation of ion pairs in the solution and natural convection. In addition, as shown in Fig. 11, the limiting current density of the electroreduction is achieved at a low electrode polarization. This means that the concentration constraints limit the electroreduction of Cu^{2+} ions.

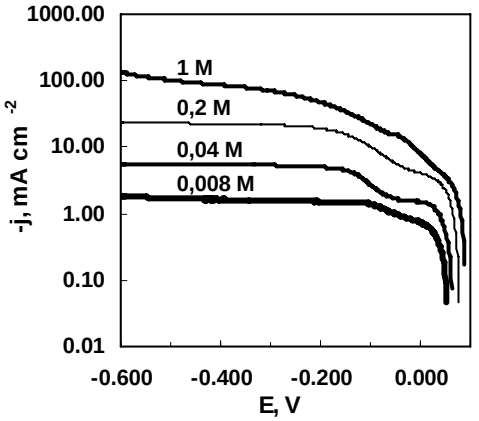

Fig. 11. Cathodic polarization curves of the Cu electrode in a solution of 0.5 M Na_2SO_4 with different concentrations of $CuSO_4$.

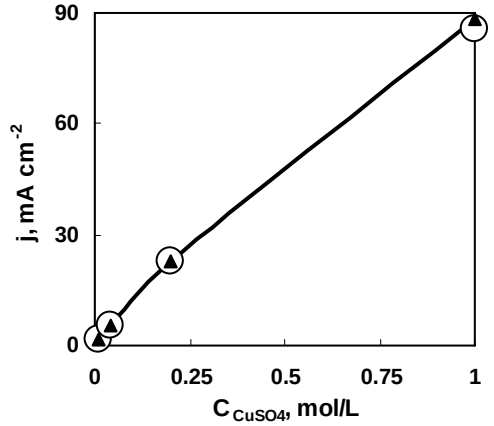

Fig. 12. Dependence of (○) the cathodic limiting current of the electroreduction of Cu(II) and (▲) the limiting current of the transmetallization of Fe with copper on the concentration of $CuSO_4$ in a solution of 0.5 M Na_2SO_4 (pH 3).

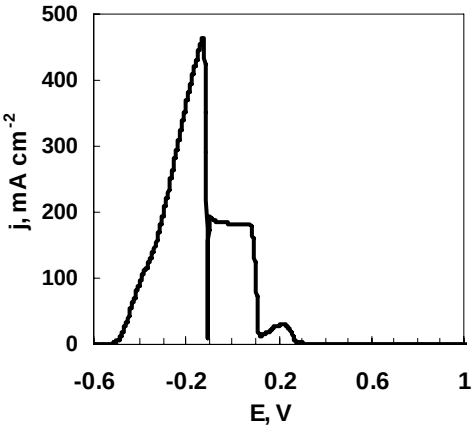

Fig. 13. Anodic Polarization curve of the Fe electrode in a solution of 0.5 M Na_2SO_4 (pH3).

The electrooxidation of iron depends on the electrolyte composition, namely, on the type of anion contained in the solution. Figure 13 shows the anodic polarization curve of the Fe electrode in a 0.5 M Na_2SO_4 (pH 3) solution. It is evident that the electrooxidation of Fe occurs at a more negative potential, and the oxidation rate achieves fairly high values (active dissolution with the formation of Fe^{2+} ions). At a potential of approximately –0.1 V, the current density sharply decreases due to the passivation of iron surface, and complete passivation of the surface occurs at potential about +0.4 V.

It is clear that the electrooxidation of Fe occurs at more negative values of the potential than the electroreduction of Cu(II). This suggests that the rate of the transmetallization depends only on the conditions of the electroreduction of Cu(II). The passivation of the surface of iron was studied using chronopotentiometric measurements of the potential of the Fe and Cu electrodes in solutions with different concentrations of $CuSO_4$. The results are shown in Fig. 14.

Fig. 14a shows that the potential of the Cu electrode fairly rapidly reaches steady state values and remains unchanged. The values of ones are close to equilibrium values. The change in the value of the iron electrode potential is caused by the transmetallization reaction that occurs in solutions containing Cu^{2+} ions. The experimental data presented in Fig. 14b show that the values of the potential of the Fe electrode correspond to the region of active dissolution of iron. In addition, the fluctuation of the Fe potential in a solution with a high concentration of $CuSO_4$ is observed. The initial values of the reaction rates represented in Fig. 12 show that the rate of transmetallization of Fe expressed in electrical units is close to the limiting current density of copper. Thus, the methods for the determination of the corrosion rates can be applied to study the modification of the surface of Fe with copper.

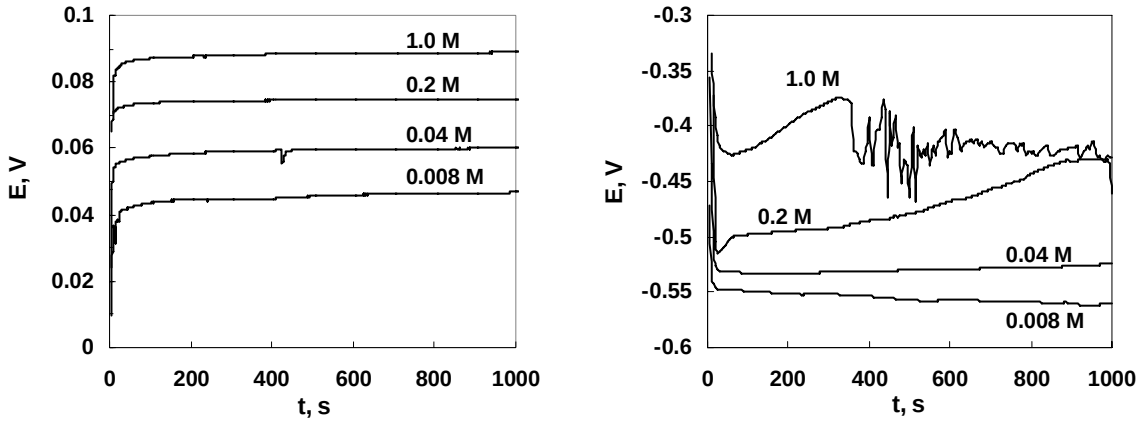

a **b**

Fig. 14. Dependence of the potential of the Cu (a) and Fe (b) electrode on the time of immersion in a solution of 0.5 M Na_2SO_4 with the different concentrations of $CuSO_4$ (pH 3).

Figure 14b shows that the value of the potential of the Cu electrode remains unchanged in the $CuSO_4$ solution for a fairly long period, and this value corresponds to the range of active dissolution of the Fe electrode. This means that the transmetallization of Fe occurs as long as copper ions are present in the solution. This situation is clearly unfavourable if we have intentions to modify only the surface of the Fe particles with copper.

Therefore, we studied additives that can be adsorbed and thereby block the surface of iron and stop the penetration of transmetallization reaction into the metallic phase of the Fe particles.

The glycerol dilaurate and block copolymer have an ability to stabilize nanoparticles in aqueous and non-aqueous liquids; therefore, it is appropriate to study their effect on the modification of Fe with copper. It is found that all the additives under study decrease the rate of the active dissolution of iron and increase the polarization only at higher current densities than the values of the limiting diffusion currents of Cu(II); that is, the modification of the surface of iron with copper in the presence of surfactants is also limited by the rate of the electroreduction of Cu(II). It could be concluded that the used surfactants do not completely prevent the cementation reaction; they only decrease its rate.

3.3. Estimation of Fe particles corrosion rates in the rapeseed and SAE 10 mineral oils

Spectrophotometric microanalysis for the determination of Fe (II)/Fe(III) in the presence of sulfosalicylic acid was applied. Corrosion of synthesized Fe particles in the oil phase was initiated by mixing suspensions in the open tube for fixed period of time from 1 to 5 minutes. After 24 hours Fe particles/iron oxide were separated from the oil phases and thoroughly washed with heptane.

Figure 15 shows the fraction of oxidized Fe in the RO and MO suspensions containing surfactants and at various agitation durations. Fe-particles in course of reduction by $NaBH_4$ are almost completely oxidized in the RO with OS and the MO with FVE, irrespectively of suspension blending duration. In the cases of RO+OS+Fe and MO+FVE+Fe suspensions, the corrosion rates of Fe correlate with particle sizes, i.e. the lower the Fe particle sizes, the larger contact area with the corrosive environment and the faster corrosion of Fe (up to full oxidation) is occurred. Although the size distribution of Fe particles in the RO with ENB and GLY are sufficiently similar (see Fig. 9a), the corrosion rates of Fe are totally different (see Fig. 15a). This can be explained by the composition of produced suspensions; i.e. the combination of RO/MO+surfactant induces or reduces the oxidation rate of Fe particles. The ENB surfactant provides the best protection against corrosion of Fe, but the oxidized amount of Fe significantly increases by the increasing of agitation duration from 1 to 5 minutes. RO+GLY composition maintains a uniform oxidized Fe content, irrespectively of the blending duration.

Corrosion rates of Fe particles in the SAE phase strongly depend on the suspension blending duration, i.e. the time of exposure to the air (Figure 15b). Increase the agitation duration of MO+ENB suspension from 1 to 5 minutes results the slight increase in fraction of oxidized Fe particles from 10 to 30 %. Meanwhile, in the MO+OS suspension corrosion rate of Fe particles significantly depends on a contact time with the air. It should be noted that OS surfactant provides the effective protection against corrosion, if mixing in a minute, but by increasing the blending duration from 1 to 5 minutes the preservation mechanism by adsorbed OS film becomes ineffective. As it is seen in Fig. 9b, the size distribution ranges of Fe particles in MO with GLY and without surfactant are sufficiently similar. However, the fraction of oxidized Fe particles in MO is lower than that in the suspension with GLY. It is obvious that MO+GLY G2L composition affects chemically Fe particles and increases their oxidation rate.

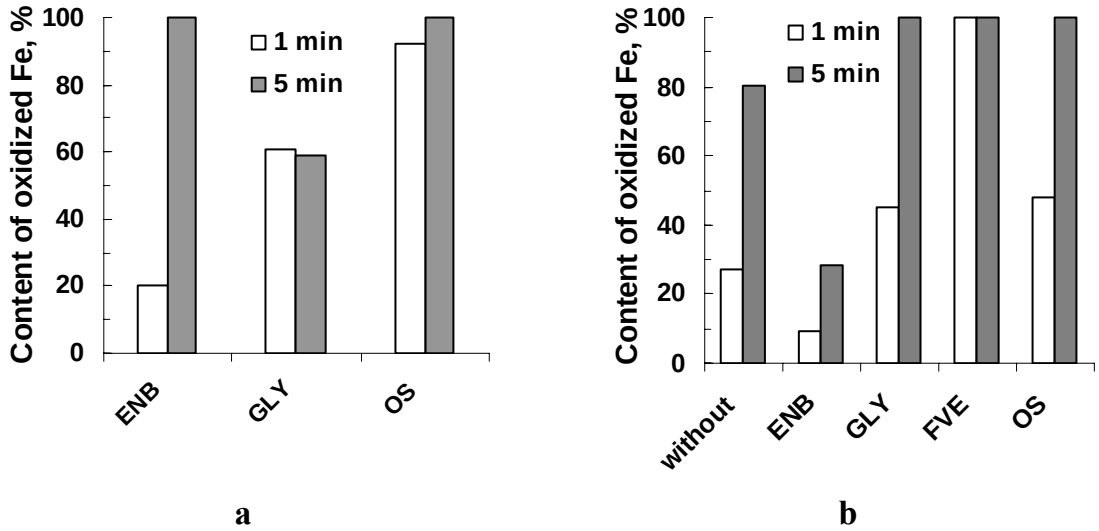

Fig. 15.The fraction of oxidized Fe (%) in: (a) rapeseed and (b) SAE 10 mineral oils with different surfactants and agitation duration. $NaBH_4$ reducing agent is used for preparation of Fe particles.

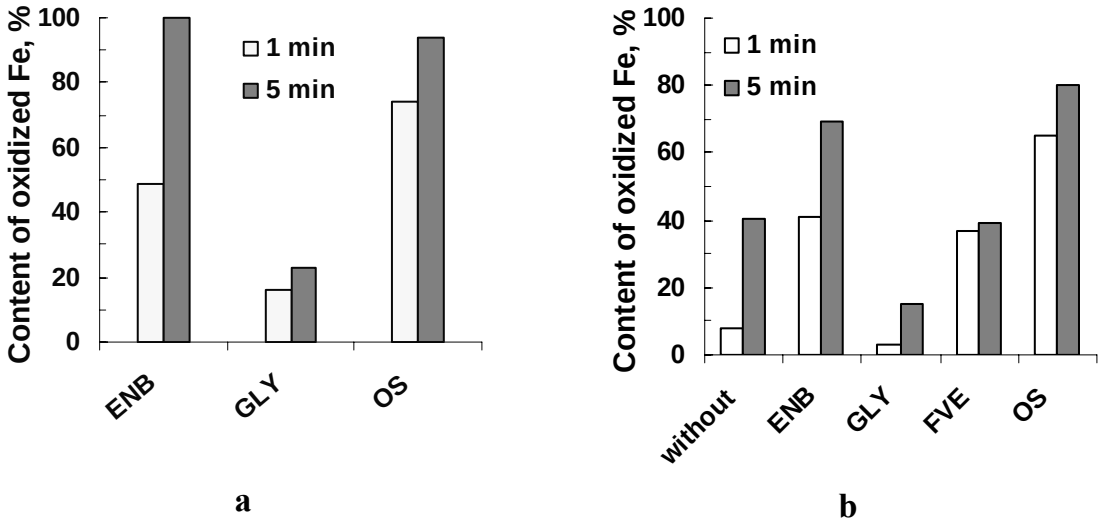

Fig. 16. The fraction of oxidized Fe (%) in: (a) rapeseed and (b) SAE 10 mineral oils with different surfactants and agitation duration. $LiBEt_3H$ reducing agent is used for preparation of Fe particles.

Fig. 16 shows the fractions of oxidized Fe particles in the RO and MO suspensions with different surfactants and agitation duration. In RO/MO+ENB suspensions the corrosion rate of Fe significantly increases with the increase of blending duration. The results presented in Fig. 16a show that the corrosion rate of Fe correlates not only with the Fe particle sizes, but with the overall composition of suspensions.

The study of Fe corrosion in the RO with OS demonstrates that this composite system enhances the corrosion rate of Fe particles irrespective on their sizes and the blending duration. The fraction of oxidized Fe particles in RO+GLY suspension is within ~23 %, irrespectively of Fe particle sizes and the blending duration. The corrosion rates of Fe associated with the range of Fe particle sizes and stabilization mechanism of GLY surfactant.

The results presented in Figure 16b shows that in MO+GLY suspension the fraction of oxidized Fe particles remains within 15 %, whereas in MO+FVE suspension

the fraction of oxidized Fe remains uniform (~38 %), independently of agitation duration and sizes of Fe particles.

Summarizing, the corrosion rate should be correlated with the Fe particle size. However, it is emphasized that in some cases the stabilization mechanism of surfactant becomes the most important. As it is seen in Figs. 15 and 16, the fraction of oxidized Fe increases with increasing agitation duration (contact with air duration) and decreasing sizes of Fe particles.

It is noted that using $NaBH_4$ and $LiBEt_3H$ for the synthesis of Fe-particles the fractions of oxidized Fe particles in the rapeseed oil are quite similar. Meanwhile, in case of reduction by $LiBEt_3H$ in the MO suspensions the fraction of oxidized Fe particles is lower, than in case of reduction by $NaBH_4$. In addition, in most cases, irrespective of used oil medium, but depending on the blending duration, the OS surfactant is not effective for protection of Fe particles against corrosion.

3.4. Tribological investigation

3.4.1. Characterization of the oils and oil suspensions

The data of kinematic viscosity measurements are presented in Fig.17. These data further are used for quantitative description of tribological results. The viscosity is governed mostly by the nature of the oil and surfactant. The viscosity in the presence of Fe particles does not increase sufficiently and it is in accordance with Einstein theory applied for the emulsions with low volume fraction of solid particles. The RO with Fe particles and surfactant gave a slight increase in oil viscosity and the anomalous increase in viscosity of the MO was detected in the presence of surfactant OS (Fig. 17), that is caused probably by the chemical interactions between OS surfactant and MO.

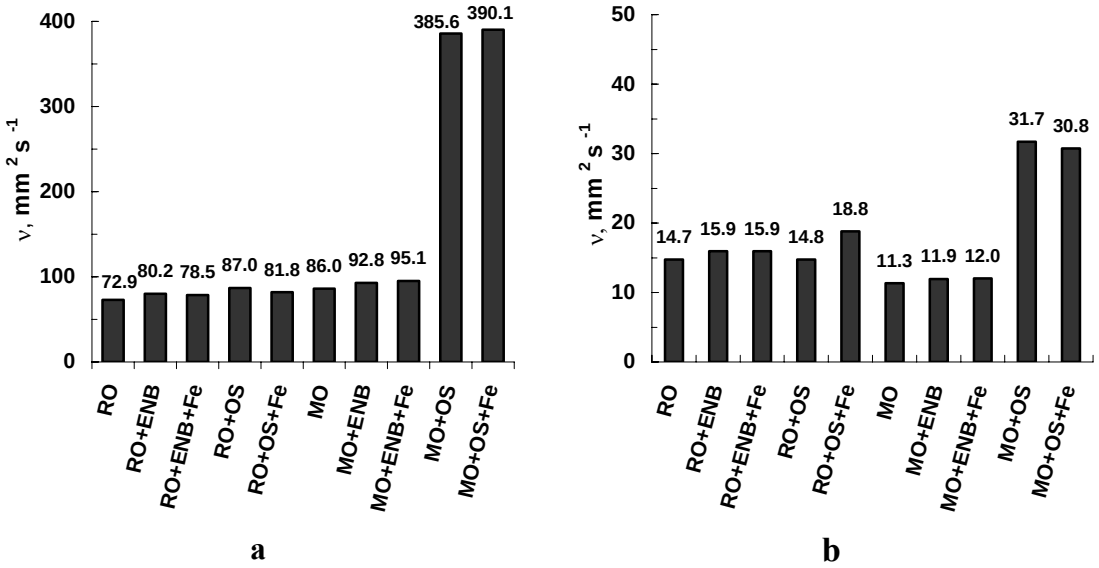

Fig. 17. Results of the kinematic viscosity measurements for the rapeseed and mineral oil solutions at 22 ^{0}C (a) and 75 ^{0}C (b).

3.3.2. Four-Ball Wear tribotests under high loads

The RO and MO solutions with different combination of surfactants, and Fe particles were prepared. Moreover, pure BO and BO with well-known 0.5 wt % glycerol monooleate additive was used as references. For convenience, a list of the prepared oil solutions and its labcodes are listed in Table 3.

Table 3. Tested oil suspensions (in wt %)

Test samples	Labcode
Base oil	BO
Base oil + 0.5 % glycerol monooleate	BO+GMO
Rapeseed oil + 0.5 % antioxidant	RO
Rapeseed oil + 0.5 % antioxidant + 0.5 % OS-20 + **0.1 % Fe** +4.4 % H_2O	RO + OS + Fe
Rapeseed oil + 0.5 % antioxidant + 0.5 % OS-20+4.4 % H_2O	RO + OS
Rapeseed oil + 0.5 % antioxidant + 0.5 % ENB 90R4 + **0.1 % Fe** + 4.4 % H_2O	RO + ENB + Fe
Rapeseed oil + 0.5 % antioxidant + 0.5 % ENB 90R4+4.4 % H_2O	RO + ENB
SAE 10 + 0.5 % antioxidant	MO
SAE 10 + 0.5 % antioxidant + 0.5 % OS-20 + **0.1 % Fe** + 4.4 % H_2O	MO + OS + Fe
SAE 10 + 0.5 % antioxidant + 0.5 % OS-20+4.4 % H_2O	MO + OS
SAE 10 + 0.5 % antioxidant + 0.5 % ENB 90R4 + **0.1 % Fe** + 4.4 % H_2O	MO + ENB + Fe
SAE 10 + 0.5 % antioxidant + 0.5 % ENB 90R4+4.4 % H_2O	MO + ENB

The average coefficient of friction (COF) and the wear scar diameter measured after the Four-Ball Wear tests on various oil suspensions are shown in Figs. 18 and 19. The lowest COF was obtained on the unmodified RO irrespectively of the applied loads. The addition of Fe particles to this oil resulted in the some increase in COF. Moreover, the results show that the COF is lower than on the base oil containing GMO additive. Interestingly, at 75 °C, the viscosity of the RO with OS+Fe particles is about 40 % higher, and the average COF increases by the same order. Thus, the increase in COF can be attributed to higher viscous drag in the contact.

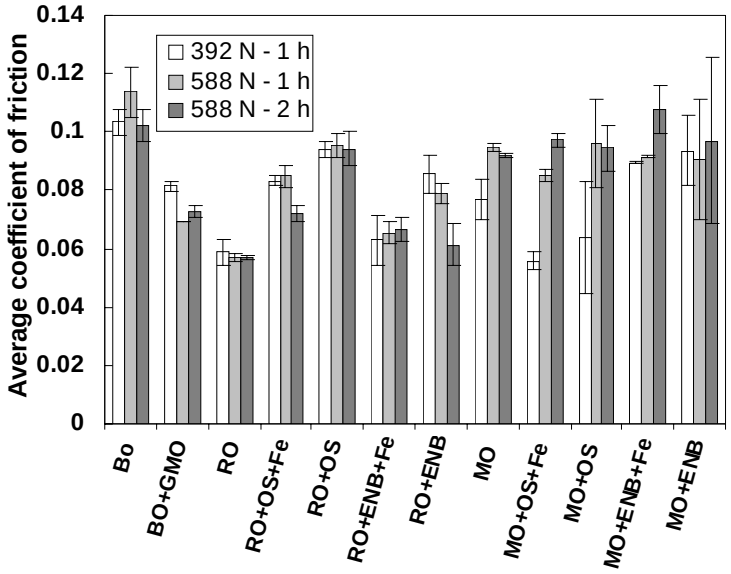

Fig. 18. The average coefficient of friction recorded in the rapeseed and mineral oil suspensions.

The surfactant ENB does not change viscosity (Fig. 17), and the increase in COF is mostly governed by the presence of sub-micron Fe particles. Focusing on the obtained data, it can be concluded that Fe particles of 165-340 nm size range reduce COF more effectively than Fe particles of 50-120 nm size. Fe particles of the range 50-120 nm size do more asperities interaction as abrasive material than bigger size particles (165-340 nm).

The COF values obtained for MO and for combinations of surfactant+Fe particles are shown in Fig. 18. The addition of OS+Fe particles has a significant reduction of COF at 392 and 588 N loads for 1 hour test duration. With the addition of ENB+Fe particles, a

slight decrease in COF was detected. This indicates that for MO the addition of particles is beneficial for friction reduction as well.

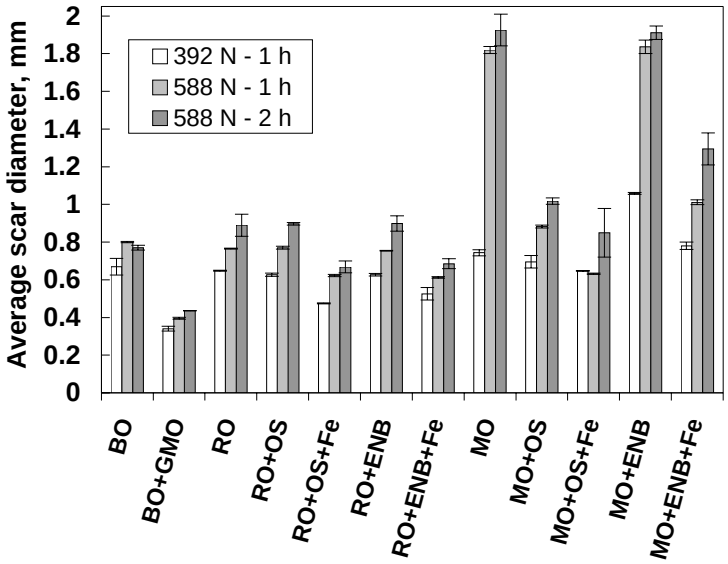

Fig. 19. The obtained average scar diameter on the top of three balls measured by the light optical microscope.

The measured average wear scar diameters obtained on the steel balls after Four-Ball Wear tests are shown in Fig. 19. There is a significant improvement in the anti-wear property of the RO and MO by the addition of Fe particles irrespectively of the surfactant used. Especially, the anti-wear improvement for mineral oil at 588 N is excellent. The MO+OS+Fe gave the best anti-wear performance whereas for the RO the wear improvement was similar with both the surfactants.

The examples of damages on the balls after the test obtained on different RO solutions are shown in Fig. 20. The wear scar with pure RO is around 650 μm whereas with OS+Fe particles it was 480 μm (at 26 % less) and with ENB+Fe particles was slightly more at 490 μm (at 25 % less). Irrespectively of the size range of the Fe particles there was a significant improvement in the anti-wear property of the RO. At higher load of 588 N, the wear reduction was lower at about 20 %.

The 588 N forces on the three point contacts and it is probably a harsh test condition. One more aspect is the release of new Fe particles as wear debris. The steel balls as they wear release fresh Fe particles into the oil. During high wear tests, the concentration of Fe particles can be very dynamic and therefore the wear rate becomes depend on their local concentrations. Under such circumstances the agglomeration and segregation of particles could be an issue causing a drop in the anti-wear performance.

The same analysis of wearing data in the MO shows clearly, that the OS-Fe particle combination gives the best anti-wear property. At 392 N, the wear reduction by ENB+Fe particles was 4 % whereas with OS-Fe particles it is 17 %. At high loads, the wear protection is improved even more with OS-Fe showing reduction in the wear scar size by 64 % and for ENB+Fe – by 41 %. Both surfactants+Fe particles caused some layers on the steel balls (see Fig. 21), and these reaction layers were more evident using surfactant OS. It is hypothesized that surfactants with Fe particles and the MO form some kind of active complexes. Further surface analysis of these reaction layers is necessary and it is possible that these layers possess good extreme pressure (EP) property as evidenced during 588 N load test.

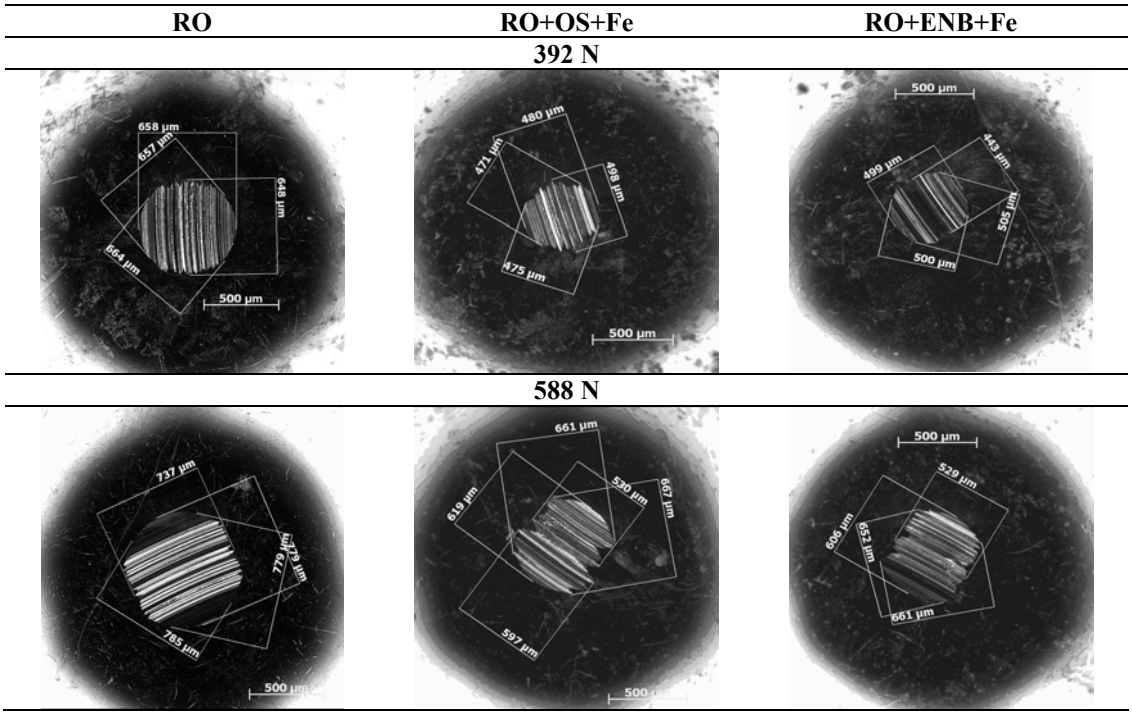

Fig. 20. Light optical micrographs of wear scars on the balls after Four-Ball Wear test on the rapeseed oil solutions.

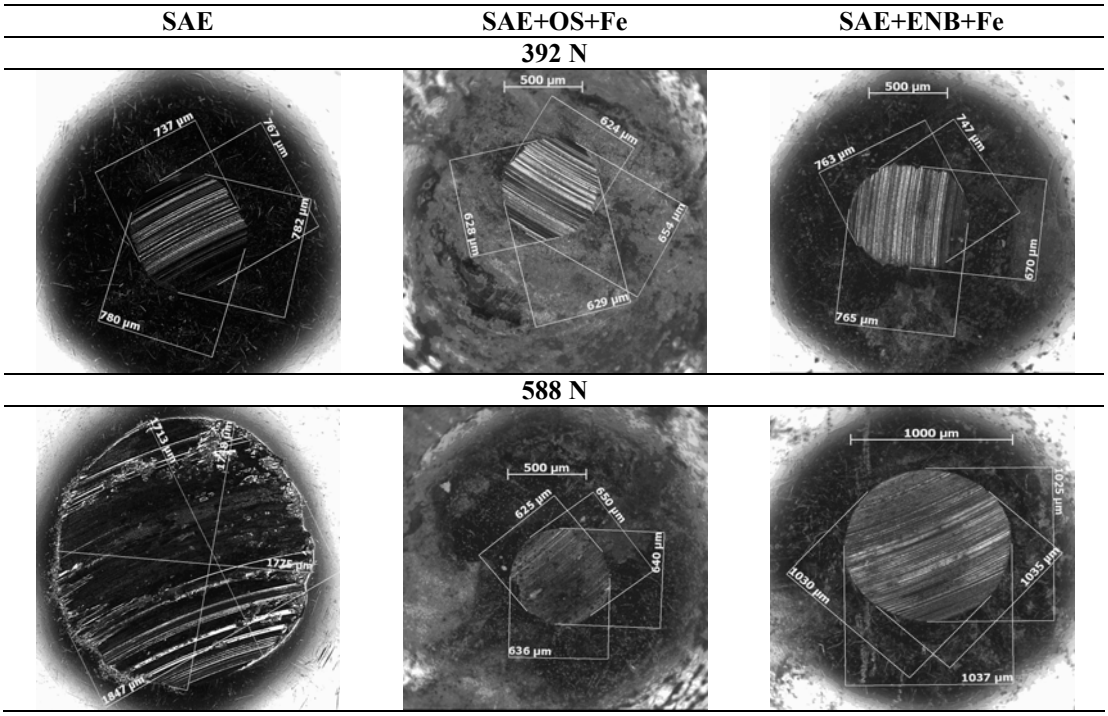

Fig. 21. Light optical micrographs of wear scars after Four-Ball Wear test on the mineral oil solutions.

In the Four Ball set-up, the three point contacts give rise to the frictional torque. This frictional dissipated energy contributes to the wear loss. One way of judging the lubricant performance is estimating the approximate wear rates by energy approach.

The linear speed at the three point contacts is 0.46 m/s. Thus, each ball covers a distance of 1650 m and the three balls cover a total of 4950 m. This distance multiplied by average friction force and test duration should give an estimated dissipated energy. A of wear loss (measured as area of the scar) versus dissipated energy for the mineral oil with different surfactant and Fe particles is shown in Fig. 22. The MO without Fe

particles shows a high slope indicating high wear rate. The three data points do not fit linearly which indicates a change in wear mechanism at high load (588 N for 1 and 2 hours). The MO containing surfactant OS and Fe particles gives smallest wear rate.

A visible trend means that the MO suspension with smaller Fe particles (the range size of 50-120 nm) shows the best anti-wear performance. Finally, the MO with ENB surfactant and Fe particles also shows a large improvement in wear rate when compared with the unmodified mineral oil. The slopes obtained on the suspension of MO+ENB+Fe and MO+OS+Fe are much lower than for the unlubricated metallic contacts.

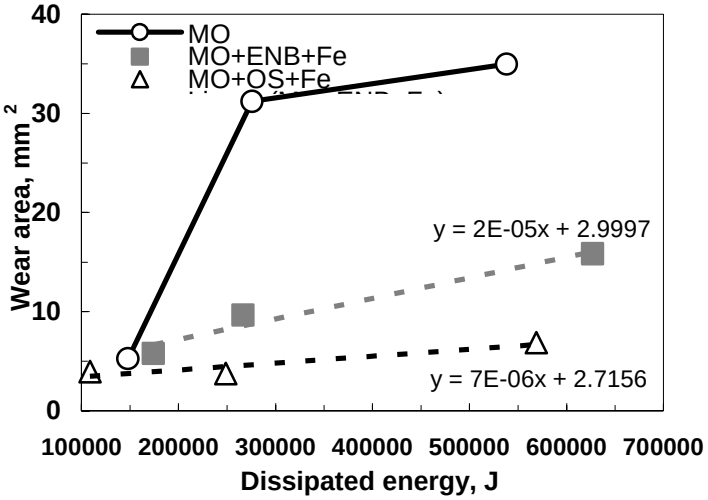

Fig. 22. Wear area versus dissipated energy data for the mineral oil with/without Fe particles.

The wear loss (in terms of wear area) versus frictional dissipated energy for the RO with different combinations of surfactant + Fe particles is shown in Fig. 23. Once again the observable reduction of wear rate of the steel balls is determined. In this case, the RO+OS+Fe suspension gives the best wear reduction followed by ENB+Fe particles. However, the degree of improvement is not much as in the case of the MO, but the smaller Fe particle size obtained with OS surfactant gave the least wear rate.

The possible explanation for improvement the lubricity and anti-wearing properties can be solely based on the surfactant+Fe particle combination. The positive effect of the presence of Fe particles of sub-micron size could be explained by formation of tribochemical reaction products or tribofilms by Fe particles.

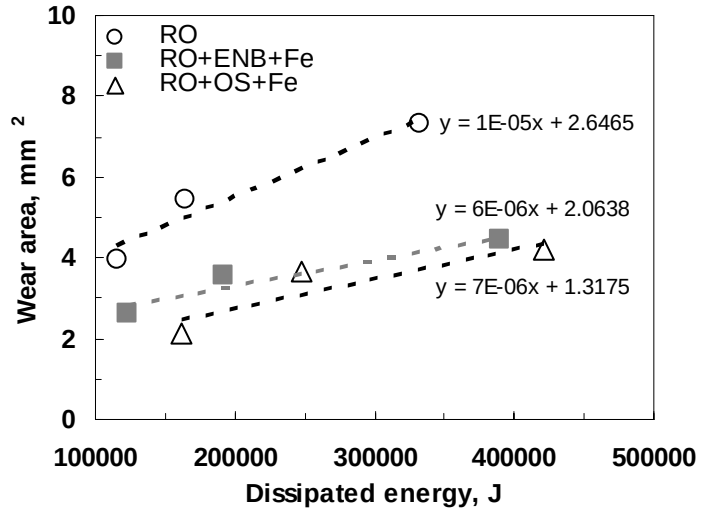

Fig. 24. Wear area versus dissipated energy data for the rapeseed oil with/without Fe particles.

3.3.3. MUST tribotests under low loads

The tribological evaluation based on MUST method was performed under low contact pressures and slow speed thus allowing a direct measurement of the frictional response with limited wear. The graphs of the average coefficients of friction versus dimensionless term of Sommerfeld number recorded during the reciprocating sliding tribotests using the MUST microtribometer are shown in Fig. 24. For the convenience and clarity, the data presented in Fig. 24 are arranged by type of oils. The Sommerfeld number combines sliding velocity (V), load (L), lubricant viscosity (ν) and is calculated as $S = \nu V/L$. It is assumed that the sliding velocity remains nearly constant although in the reciprocating test the directionality and magnitude of velocity changes.

For rapeseed oil without Fe particles the values of COF are ranged between 0.124-0.128 dependently on the sliding velocity and load (Fig. 24 a), and adding of Fe-particles into suspension does not change COF sufficiently: 0.124 at lowest $\nu V/L$ and then increased to 0.136 at the highest $\nu V/L$.

The similar effect on the COF caused by the presence of Fe particles in RO was obtained in the presence of surfactant OS: for RO+OS+Fe suspension was recorded in the similar range 0.121–0.139, whereas for RO+OS suspension the COF values changed in the range of 0.099–0.112. Focusing on the results obtained during the sliding tribotests, it can be concluded that Fe particles do not cause the significant change in the friction or lubricity of the rapeseed oil. However, addition of OS surfactant can improve tribological characteristics of rapeseed oil in comparison with the influence of surfactant ENB with or without Fe particles.

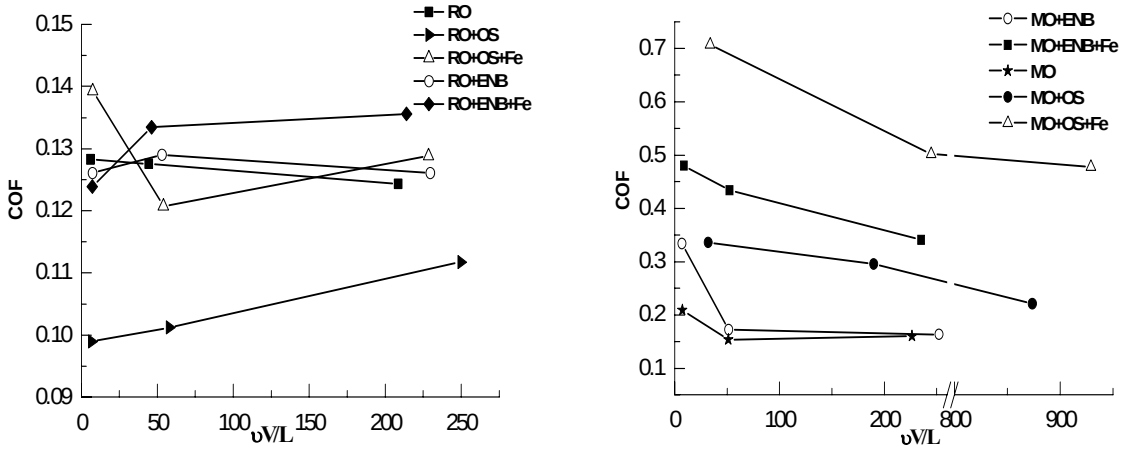

Fig. 24. The average coefficient of friction (COF) recorded under bidirectional sliding conditions on (a) the rapeseed oil (RO), and (b) the mineral oil (MO). Relative standard error ≤ 7 %.

In the case of the mineral oil containing surfactants or surfactants with Fe particles the values of COF are increased (Fig. 24 b). At low $\nu V/L$, in the presence of OS and Fe particles the average COF comparing to non-modified mineral oil increase from 0.209 to 0.707. Hereupon, the MO+OS+Fe and MO+OS suspensions showed unusually high viscosity at 22 °C (Fig. 17a), but only on the MO+OS+Fe suspension the highest friction values was obtained. In general, the mineral oil containing Fe particles exhibited the coefficient of friction more than 0.35. Thus, under low loads the modified mineral oil with Fe particles+surfactant demonstrated high friction.

Comparing these two lubricating oils, it can be concluded that the rapeseed oil with or without surfactant/iron particles gives the lower coefficient of friction in comparison with mineral oil investigated.

Comparing the influence of two surfactants on friction in rapeseed and mineral oils it is clear that for the rapeseed oil, both ENB and OS surfactants have no effect on the friction behaviour, whereas both ENB and OS with Fe particles in mineral oil suspensions adversely influence on the COF: it increased up to 0.477-0.707 comparing with 0.153-0.209 in the blank MO.

An insight on the mechanisms of friction in the presence of iron particles can be understand by analyzing the friction loops (tangential force versus distance) obtained during the reciprocating sliding tests. The fluctuations in the friction force arise due to different effects like third bodies, material/phase effects, and topographical effect. On the same substrate, if Fe particles should be present in the contact, the fluctuations in the friction loops could get some additional information. The mineral and rapeseed oil suspensions with OS surfactant were selected, because both these suspensions contained Fe particles of similar size. A comparison of friction loops for the mineral and the rapeseed oils with and without Fe particles/surfactant OS under different loads and speeds is shown in Fig. 25 and 26.

The friction loops recorded for non-modified RO, modified RO+OS surfactant, and modified RO+OS+Fe particles are shown in Fig. 25. There is no significant difference between the friction loops in terms of fluctuations in the tangential force. Even the area of the friction loops; i. e. dissipated energy is similar in all the cases. This can become a case under two conditions: (i) when Fe particles are pushed out of the contact zone, or (ii) when Fe particles are covered by the rapeseed oil and the particles roll and slide without abrasion that results in the same friction as unmodified rapeseed oil. The exact cause for this interesting behaviour has to be further investigated.

The friction loops recorded during sliding tests on modified MO with OS surfactant, with/without Fe particles are shown in Fig. 26. The friction loops of non-modified MO show no fluctuations in the tangential force. However, the friction loops of MO+OS and MO+OS+Fe suspensions exhibited large fluctuations. The friction loops of MO+OS suspension are „noise“-like to stick-slip behaviour. In the case of MO+OS+Fe suspension, the friction loops also exhibited an absolute in the area of the loop (dissipated energy) along with stick-slip type of fluctuations. The change in the friction loops characteristics and overall increase in the dissipated energy confirm the presence of Fe particles in the contact. Surprisingly, the friction loops recorded on MO+OS+Fe at 900 mN (Fig. 26 c) showed less fluctuations. The decrease in friction force/dissipated energy at 900 mN and higher sliding speed of 2.6 mm/s could be due to the expulsion of Fe particles from the track and less chance for other Fe particles to settle in the wear track.

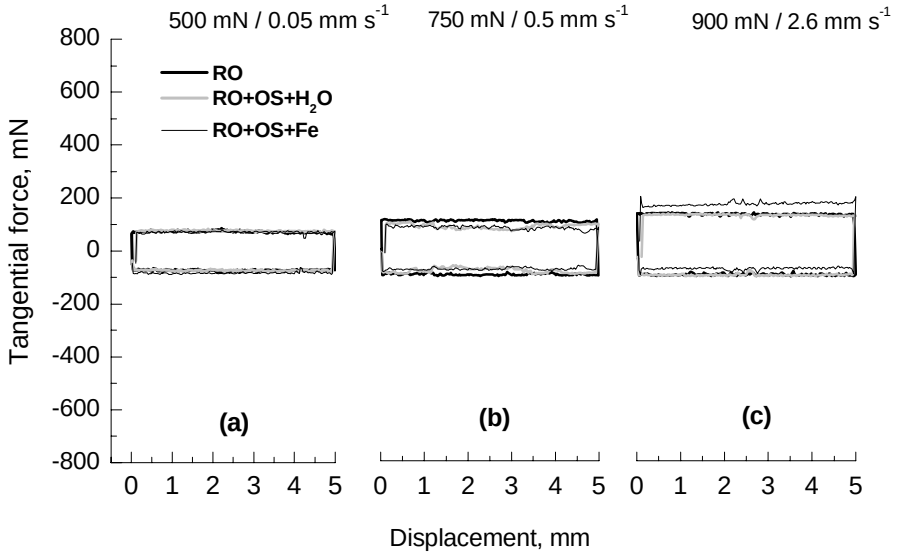

Fig. 25. Representative friction loops for 50th cycle on non-modified RO, modified RO+OS+H_2O, and RO+OS+Fe under various normal loads and sliding speeds (shown near every friction loop). Conditions: (*a*) normal load 500 mN, sliding speed 0.05 mm/s; (*b*) 750 mN, 0.5 mm/s and (*c*) 900 mN, 2.6 mm/s.

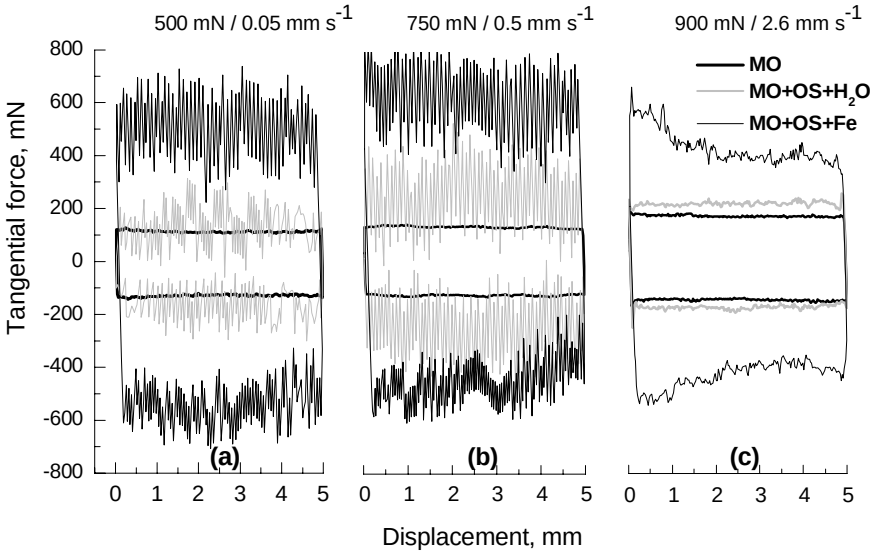

Fig. 26. Representative friction loops for 50th circle on non-modified MO, modified MO+OS+H_2O, and MO+OS+Fe under various normal loads and sliding speeds (shown near every friction loop). Conditions: (a) normal load 500 mN, sliding speed 0.05 mm/s; (b) 750 mN, 0.5 mm/s and (c) 900 mN, 2.6 mm/s.

4. CONCLUSIONS

1. The synthesis of iron particles was studied in aqueous and reverse micelle in rapeseed and mineral oils. Iron particles have been prepared by the reduction with $NaBH_4$ and $LiBEt_3H$ in presence of surfactants. In all investigated cases obtained Fe particles are polydispersed. Using $LiBEt_3H$ reducing agent the smallest size distribution of Fe particles (10-80 nm) was obtained in water. In the rapeseed and SAE 10 mineral oil suspensions the size distribution varies in a wide 50-955 nm range, depending on the used surfactants. Based on XRD pattern, the dominating structure {110} of body centered cubic lattice is formed in course of synthesis using $NaBH_4$.
2. The resulting size of Fe-particles synthesized in water (with and without surfactants) correlates with obtained values of open circuit potential (OCP): the more negative OCP, the obtained Fe-particles are bigger. The sizes of Fe-particles synthesized in water or oil without surfactants using $LiBEt_3H$ are less than using $NaBH_4$ because of electrochemical factors. However, by varying oils and surfactants it is possible to obtain opposite results: smaller Fe-particles were obtained using $NaBH_4$ than $LiBEt_3H$. It is explained by the simultaneous influence of electrochemical and steric repulsion stabilization factors, and the last one becomes dominating in some cases.
3. The transmetallization of Fe by copper occurs as long as copper ions are present in the solution. The used surfactants for iron particles stabilization do not prevent the cementation reaction; they only decrease copper ions reduction reaction.
4. The corrosion rates of Fe particles in the rapeseed and SAE 10 mineral oils depend not only on the particle sizes but also on the surfactant and the composition of produced suspension.
5. The results obtained at high loads showed that in the presence of Fe and Fe modified by Cu particles in the rapeseed and mineral oils cause little change in the average coefficient of friction but result in marked improvements in the anti-wear property. The anti-wear enhancement on the other hand is attributed to tribofilm formation and superior load bearing capability of the modified oil. It was noticed that a low concentration of Fe particles, such as 0.1 wt %, is sufficient to improve anti-wear properties of both the rapeseed and mineral oils irrespectively of used surfactant.
6. Under slow reciprocating sliding conditions the results show that both OS-20 and ENB 90R4 surfactant addition have no effect on the friction/lubricity properties of the rapeseed oil, whereas cause the negative effect (increase in friction) in the case of the mineral oil. The friction loops obtained with unmodified and modified rapeseed oil were quite similar. It is assumed that the Fe particles are covered by rapeseed oil and its slide without abrasion resulting in the same coefficient of friction as for oil without additives. The difference in the friction loops of unmodified and modified mineral oil was strikingly evident. The friction loops under slow sliding speeds and low loads were characterized with large stick-slip type of fluctuations and overall increase in the dissipated energy. This could be attributed to the abrasion of the steel disc by the iron particles. However, at higher sliding speed, the fluctuations were not visible which could be due to the expulsion of particles from the contact.
7. The SAE+ENB+Fe (produced by reduction $NaBH_4$) and SAE+FVE+Fe (produced by reduction $LiBEt_3H$) suspensions are perspective for further development due to promising characteristics: the size distribution of obtained Fe particles, corrosion resistance and tribological performance.

The list of Original publications by the Author

Article in journals referenced in "ISI Web of knowledge" data base:

1. **T. Maliar**, J. Bozenko, H. Cesiulis, I. Prosycevas. Electrochemical Aspects of the Synthesis of Iron Particles, *Materials science,* ISSN 1392-1320, **2012**, Vol. 18, (already accepted to press).

2. H. Cesiulis, **T. Maliar**, S. Asadauskas. Modification of Iron Particles with Copper for Their Subsequent Use in Tribosystems, *Surface Engineering and Applied Electrochemistry*, **2011**, Vol. 47, No. 3, pp. 225–231. ISSN 1068-3755.

3. J. Padgurskas, R. Rukuiža, R. Kreivaitis, A. Kupčinskas, V. Jankauskas, H. Cesiulis, **T. Maliar**, I. Prosyčevas. Tribological properties of mineral oils modified with metallic nano-particles. *Proceedings of the 5th International Scientific Conference BALTTRIB'2009*, 19-21 November, **2009**, Kaunas, Lithuania, pp. 69-76. ISSN 1822-8801.

4. **T. Maliar**, S. Achanta, H. Cesiulis, D. Drees. Effect of iron micro-/nano-particle additives on tribological behavior of lubricating oils. *Proceedings of the 5th International Scientific Conference BALTTRIB'2009*, 19-21 November, **2009**, Kaunas, Lithuania, pp. 77-82. ISSN 1822-8801.

Published contributions to academic conferences:

1. **T. Maliar**, J. Boženko, H. Cesiulis, I. Prosyčevas. *20th International Baltic Conference Materials Engeneering 2011,* 27-28 October **2011**, Kaunas, Lithuania.
2. J. Boženko, **T. Maliar**, H. Cesiulis, *Chemistry and Technology of Inorganic Materials*, 27–28 April **2011,** Kaunas, Lithuania.
3. J. Padgurskas, **T. Maliar**, R. Kreivaitis, A. Kupčinskas, H. Cesiulis, *5th International Conference on Materials Science and Condensed Matter Physics and Symposium „Electrical Methods of Materials Treatment"* in memoriam of acad. Boris Lazarenko, 13-17 September **2010**, Chisinau, Moldova.
4. D. Drees, **T. Maliar**, S. Achanta, H. Cesiulis, *Society of Tribologist & Lubrication Engineers 2010 Annual Meeting & Exhibition*, 16-20 May **2010**, Las Vegas, USA.
5. J. Boženko, **T. Maliar**, H. Cesiulis. *The 15th Annual International Research Conference for Students and Young Researchers on Chemistry and Chemical Technology*, 07 May **2010**, Vilnius, Lithuania.
6. **T. Maliar**, J. Boženko, H. Cesiulis, S. Asadauskas, I. Prosyčevas. *Lithuanian Conference „Materials Engineering'2009",* 20 November **2009**, Kaunas, Lithuania.
7. **T. Maliar**, S. Achanta, H. Cesiulis, D. Drees. *5th International Conference BALTTRIB'2009,* 19-21 November **2009**, Kaunas, Lithuania.
8. **T. Maliar**, S. Asadauskas, H. Cesiulis. *The International Conference dedicated to the 50th anniversary from the foundation of the Institute of Chemistry of the Academy of Sciences of Moldova,* 26-28 May **2009**, Chisinau, Moldova.
9. **T. Maliar**, S. Asadauskas, H. Cesiulis. *Chemistry and Technology of Inorganic Compounds*, 22 April **2009**, Kaunas, Lithuania.

Curriculum Vitae

Education

2007-2011 - Doctoral studies at Department of Physical Chemistry of Vilnius University, Lithuania. Thesis: “Iron mezo-particle Synthesis in the Aqueous and Oil Media and Their Use in Tribosystems”.

2005-2007 - Master studies at Department of Physical Chemistry of Vilnius University, Lithuania. Thesis: “The Catalytic Effect of Dodecatungstocoboltate Mediator on the Charge Transfer Reactions”. Master degree of Chemistry.

2001-2005 - Bachelor studies of Chemistry. Department of Physical Chemistry of Vilnius University, Lithuania. Thesis: “The Catalytic Effect of Modified Graphite Electrode with Molybdophosphate”. Bachelor degree of Chemistry.

Work experience

2011/10/03-2012/02/06. Senior technician (part time) in Department of Physical Chemistry of Vilnius University, Lithuania.

2010/09/01-2011/08/31. Lecturer (part time) in Department of Physical Chemistry of Vilnius University, Lithuania.

2009/10/01-2010/08/31. Research Assistant (part time) in Department of Physical Chemistry of Vilnius University, Lithuania.

2009/02/04-2009/08/31. Research Assistant (part time) in Department of Physical Chemistry of Vilnius University, Lithuania.

2008/01/18-2009/02/01. Engineer-chemist in UAB "Vilnius Ventos Semiconductors" Chemistry Department of Microelectronics Workshop.

Fellowship

2011/05-2011/10 Chemical Engineering Department, Northeastern University, Boston, the U.S. *„Template-assisted deposition of functional materials and devices”*.
Supported by European project FP7-PEOPLE-2009-IRSES, IRSES-GA-2009-247659.

2010/10-2010/12 Chemical and Material Engineering Research laboratory (LGPM) Ecole Centrale de Paris, Paris, France. *“Electrochemical Aspects of Nano-alloys Synthesis”*.
Supported by French embassy in Lithuania (the EGIDE program).

2009/07-2009/10 Erasmus practice in company „FALEX TRIBOLOGY NV“, Leuven, Belgium. *“Formation of Iron Particles in Oils and Its Tribological Investigation as Additives in Lubricating Oils”*.
Supported by Vilnius University (the Erasmus program).

Geležies dalelių sintezė vandens ir alyvos terpėse ir jų taikymas tribosistemose

REZIUMĖ

Pastaruoju metu, aiškėja tendencija spręsti mašinų komponentų dilumo problemas į alyvas pridedant metalinių ir nemetalinių nanodalelių. Be to, metalo dalelės alyvoje atsiranda dylant mašinų komponentams, ir jų poveikio tribologinėms savybėms tyrimai yra aktualūs.

Sukurtos magnetinių Fe dalelių sintezės, modifikavimo variu ir paviršiaus aktyviomis medžiagomis vandens, augalinių ir mineralinių alyvų terpėse bei Fe dalelių korozijos greičio įvertinimo metodikos. Nustatyta sintezės sąlygų ir alyvos komponentų sudėties įtaka dalelių dydžiams. Atlikti sukurtų tepamųjų suspensijų tribologiniai tyrimai.

Fe dalelės vandenyje ir atvirkštinėse micelėse (rapsų aliejaus ir SAE 10 mineralinės alyvos terpėse) buvo gaunamos Fe^{2+} redukuojant natrio borohidridu ($NaBH_4$) arba ličio trietilborohidridu ($LiBEt_3H$) bei esant paviršinio aktyvumo medžiagoms (PAM). Visuose ištirtose terpėse gautos Fe dalelės yra polidispersiškos ir patenka į „sub-mikroninio“ dydžio intervalą. Mažiausios Fe dalelės (10-80 nm) gaunamos vandeninėje terpėje redukuojant $LiBEt_3H$. Sintezę atliekant atvirkštinėse micelėse rapsų ir SAE 10 mineralinės alyvų pagrindais gaunamas panašus Fe dalelių dydžio pasiskirstymo intervalas yra 50-955 nm ir priklauso nuo PAM.

Iš rentgeno difrakcijos spektro nustatyta, kad redukuojant Fe(II) reduktoriais vandeninėje terpėje gaunami pakankamai gryni Fe milteliai, kurių dominuojanti orientacija yra {110}.

Nulinio valentingumo geležies dalelių sintezės reakcijos redukuojant Fe(II) junginius $NaBH_4$ ir $LiBEt_3H$ savo prigimtimi yra elektrocheminės – vyksta tiesioginis elektronų perėjimas tarp reaguojančių medžiagų. Sintetintų vandenyje (su ir be paviršinio aktyvumo medžiagomis) Fe dalelių susidarymo greitis koreliuoja su atviros grandinės potencialo (AGP) vertėmis: kuo neigiamesnis AGP, tuo didesnis reakcijos greitis ir tuo didesnės Fe dalelės formuojasi. Tokiu atveju, susintetintų vandens arba alyvos fazėje be paviršinio aktyvumo medžiagų redukuojant $LiBEt_3H$ Fe dalelių dydis mažesnis, nei naudojant $NaBH_4$. Tačiau ne visais atvejais lemiantys yra tik elektrocheminiai faktoriai. Fe dalelių dydis priklauso ir nuo to, kaip PAM veikia micelių

susiliejimą: pagreitina ar sulėtina. Keičiant aliejų/alyvą ir PAM galima gauti priešingus rezultatus: mažesnės Fe dalelės buvo gautos redukuojant $NaBH_4$ nei - $LiBEt_3H$.

Buvo ištirtas Fe paviršiaus cementavimo variu procesas. Panaudotos PAM modifikavimo tirpaluose sumažina vario jonų redukcijos greitį ant geležies elektrodo paviršiaus, nes vykstant Cu jonų redukcijai kartu vyksta ir PAM adsorbcija ant geležies elektrodo. Tačiau PAM adsorbcija matyti nėra greita, ir Fe paviršius pilnai neblokuojamas.

Fe dalelių korozijos greičio įvertinimui buvo pritaikyta cheminė korozijos terpės fotometrinė analizė Fe(II) ir Fe(III). Gauta, kad Fe dalelių korozijos greitis alyvose priklauso ne tik nuo pačių dalelių dydžio, bet ir nuo visos suspensijos sudėties. Svarbiausiu faktoriumi tampa paviršinio aktyvumo medžiagų stabilizavimo mechanizmai. Tyrimų eigoje nepavyko nustatyti universalios PAM, gebančios pilnai apsaugoti Fe daleles nuo oksidacijos.

Vykdant suspensijų tribologinius tyrimus didelės apkrovos sąlygomis, nustatyta, kad trinties koeficientai tepant grynu rapsų aliejumi arba modifikuotu ENB+Fe yra mažesni, nei tepant bazine alyva su GMO priedu arba gryna bei modifikuota SAE 10 alyva. Tiriant SAE 10 mineralinės alyvos tepimo sistemas, mineralinės alyvos modifikavimas laukiamų rezultatų nedavė. Tačiau buvo nustatytas efektyvus tiriamų tepamųjų alyvų su Fe dalelėmis apsaugojimas nuo triboporos paviršiaus dilimo, tai gali būti paaiškinta tribocheminių produktų susidarymu. Tiriant nusidėvėjimo greičių duomenys, nustatyta, kad gryno bei modifikuoto rapsų aliejaus OS/ENB+Fe priedais poveikis dilimo greičiui yra ne toks ryškus, kaip tepant SAE mineraline alyva su tais pačiais priedais. Analizuojant tepamąsias sistemas mažos apkrovos sąlygomis gauti rezultatai parodė, kad Fe dalelių buvimas rapsų aliejuje neturi didelės įtakos trinties koeficientams. Tačiau OS-20 paviršinio aktyvumo medžiagos pridėjimas į rapsų aliejų žymiai pagerina tepimo aliejaus savybes, lyginant su ENB 90R4. Toks reiškinys gali būti paaiškinamas skirtingu PAM poveikiu tepamojo sluoksnio suformavimui. Tuo tarpu, SAE 10 mineralinės alyvos modifikavimas Fe dalelėmis bei PAM nepagerina alyvos tribologinių savybių.